ISSN 1062-8738, Bulletin of the Russian Academy of Sciences. Physics, 2014, Vol. 78, No. 10, pp. 1075–1080. © Allerton Press, Inc., 2014.
Original Russian Text © V.N. Nikiforov, A.E. Goldt, E.A. Gudilin, V.G. Sredin, V.Yu. Irhin, 2014, published in Izvestiya Rossiiskoi Akademii Nauk. Seriya Fizicheskaya, 2014, Vol. 78, No. 10, pp. 1330–1335.

Magnetic Properties of Maghemite Nanoparticles

V. N. Nikiforov[a, b], A. E. Goldt[a], E. A. Gudilin[a], V. G. Sredin[b], and V. Yu. Irhin[c]

[a] *Department of Low-Temperature Physics, Moscow State University, Moscow, 119991 Russia*
[b] *ANO Scientific Innovation Center for Space Rocket Hardware (NITs RKT), Moscow, 127642 Russia*
[c] *Institute for Metal Physics, Ural Branch, Russian Academy of Science, Yekaterinburg, 620041 Russia*
e-mail: nvn@lt.phys.msu.ru

Abstract—Magnetic particles of maghemite (spinel γ-Fe_2O_3) are synthesized by means of aerosol pyrolysis, making it possible to produce chemically uniform highly-dispersed single-phase materials. The magnetic properties of synthesized particles for temperatures ranging from helium temperature up to room temperature and higher are investigated using a SQUID magnetometer. The experimental curves are compared to the results from calculations performed by the Monte Carlo method. It is found that the Curie temperature is lower for γ-Fe_2O_3 nanoparticles than for bulk samples. Several parameters of the material are estimated by comparing the experimental and calculated results.

DOI: 10.3103/S1062873814100141

INTRODUCTION

Maghemite γ-Fe_2O_3 is a ferromagnetic material with a spinel structure. It is characterized by great magnetism and high residual magnetization. This material crystallizes in a spinel structure where totally oxidized ferrum ions Fe^{3+} are in the tetrahedral crystallographic position. Maghemite is common mineral on the surfaces of the Earth and Mars. It is found in corrosion products and proteins in nanostructural and in ultradispersed forms. It is also used in medicine for delivering drugs [1], in nuclear magnetic resonance tomography [2], and as a carrier of information [3].

Maghemite is not stable: if the temperature rises, it loses its magnetic properties and transforms into hematite α-Fe_2O_3 (it forms a continuous meta-stable magnetic solid solution upon heating). The temperature of its transformation depends on its prehistory: in a poorly oxidized sample, it is ~300°C; in a better oxidized sample, it can be higher than 450°C [4]. Particle size, water content, and stoichiometry also affect the transformation temperature [5–9].

Lepidocrocite dehydration or magnetite (Fe_3O_4) oxidation at temperatures lower than 300°C is a common procedure for synthesizing maghemite. Existing chemical methods allow us to synthesize different forms of maghemite: micrograins, films, or nanoparticles at sufficiently high temperatures [8, 9]. But there is a problem with all of these methods: we must separate maghemite from other accompanying phases of ferrum oxide. New chemical methods enable us to synthesize high-quality maghemite in grains, films, or nanoparticles at very high temperatures.

Due to the above factors it is difficult to measure the Curie temperature of maghemite. However, investigations performed with synthetic samples subjected to rapid heating [10] show that we may assume a Curie temperature of about 645°C for metastable maghemite. The problem can be solved by developing the new procedures for synthesizing maghemite nanoparticles that would allow us to obtain a stable form of this material. Different surface coatings are normally used for this purpose, but here we must solve a related problem: investigating the properties of the magnetic cores of passivated nanoparticles.

EXPERIMENTAL

In this work, we used γ-Fe_2O_3 particles synthesized by means of aerosol pyrolysis, which allowed us to produce chemically uniform, highly dispersed single-phase materials [11]. To prevent the aggregation of synthesized particles and stabilize their surfaces, we used a procedure for encapsulating nanoparticles inside grains of salt produced from sodium chloride, allowing us to keep the magnetic particles in nonaggregated state for long periods of time. To accomplish this, we used ferrum nitride and carbamide solutions while adding 5–20 moles of NaCl per 1 mole of ferrite. The mixture was sprayed with an ultrasonic inhaler (frequency of ultrasonic oscillations, 2.64 MHz; size of the particles generated in the aerosol, 0.5–5 μm) using a gas carrier (air) fed into a preliminarily heated furnace at a flow rate of 1300 mL/min. The procedure produced salt water-soluble microcapsules ~1 μm in size that included monodispersed nanoparticles lower than 10 nm in size. The molar ratios between the NaCl and the maghemite were 20 : 1, 10 : 1, 5 : 1, depending on the synthesis conditions.

The micromorphology of γ-Fe_2O_3–10NaCl composite was investigated with a transmission electron microscope. It was found that the composite's micro-

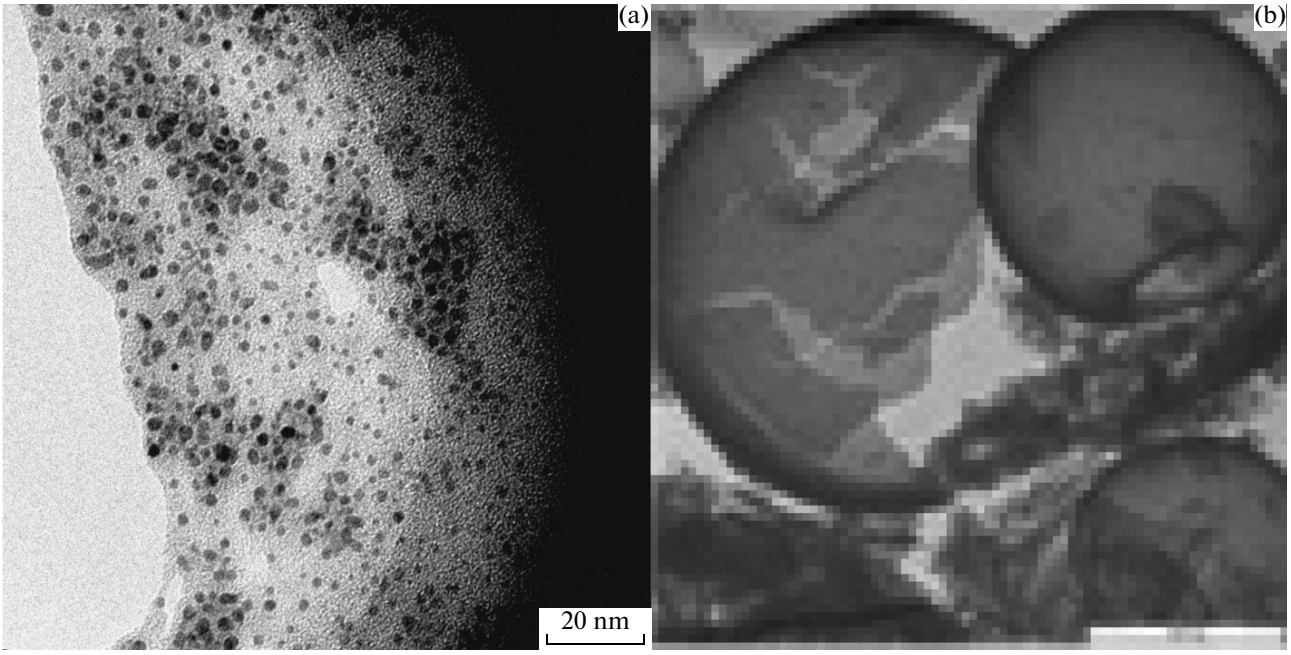

Fig. 1. Photo of a nanoparticle in a shell of sodium chloride (γ-Fe_2O_3–10NaCl). (a) Concentration of γ-Fe_2O_3–10NaCl composite in solution, 200 mg/L. The nanoparticles in the photo are <5 nm in size. (b) Initial salt capsule with γ-Fe_2O_3 nanoparticles.

spheres were hollow and their shell consisted of nanoparticles of virtually the same size (<10 nm).

If we added inert (but not toxic) diluent (sodium chloride) to the initial solution, maghemite nanoparticles formed that were encapsulated in a water-soluble matrix. The results from electron microscopy (Fig. 1) show that the sizes of maghemite nanoparticles were ~4 nm. Figure 1 shows a capsule with nanoparticles synthesized by the procedure described above. The image was obtained via transmission electron microscopy. It can be seen that the capsules are hollow and there are nanoparticles inside them. The nanoparticles are virtually identical in size (<10 nm).

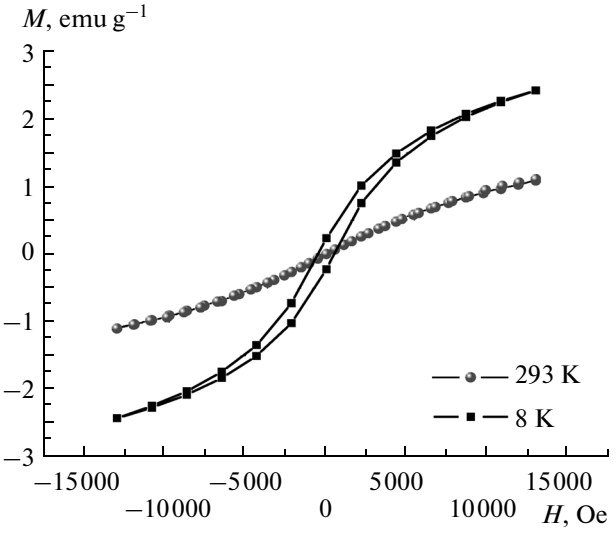

Fig. 2. Magnetic field dependences of maghemite nanoparticles at room temperature and 8 K.

In this work, we investigate the magnetic properties of γ-Fe_2O_3 nanoparticles in a hydrochloric acid matrix using a SQUID magnetometer. Each sample we examine is put into a special clean quartz ampoule with a diameter of 5 mm that is then mounted along the anti-Dewar vessel's axis in the magnetometers' chamber, the temperature of which can be varied from 2.2 up to 350 K. A uniform magnetic field of up to 20 kOe is generated by a niobium–titanium pipe in the main helium tank.

Magnetization curves $M(H)$ for nanoparticles synthesized at a temperature of 650°C (in the hot zone of a furnace) are measured at 8 and 293 K. From Fig. 2, we can see that the abovementioned curves display behavior typical of superparamagnetic nanoparticles: there is neither a hysteresis above 80 K nor saturation for $M(H)$ until strong magnetic fields are attained. In our experiments, we saw no saturation up to fields of 20 kOe. Such behavior, which is typical of superparamagnetic nanoparticles, is consistent with the results from Mössbauer spectroscopy [12], verifying that maghemite nanoparticles (with sizes of <5 nm) are present in the same samples. This means that maghemite is formed at pyrolysis temperatures of 650–700°C (the temperature in the hot zone of our reactor). It is well known that one problem in working with bulk maghemite is that it transitions into a nonmagnetic phase (either hematite or α-Fe_2O_3) [4–10].

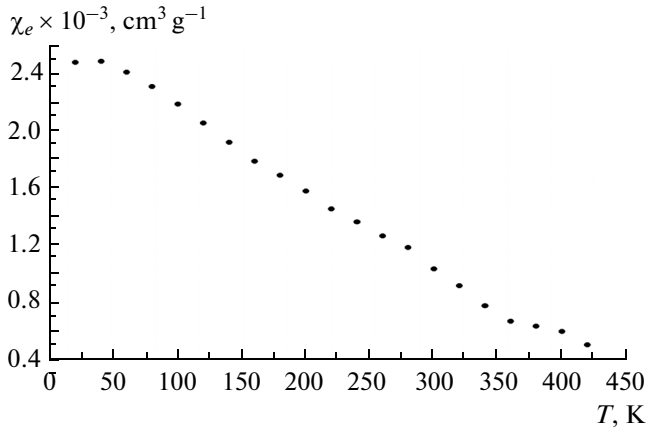

Fig. 3. Relationship between magnetic susceptibility and temperature for maghemite nanoparticles.

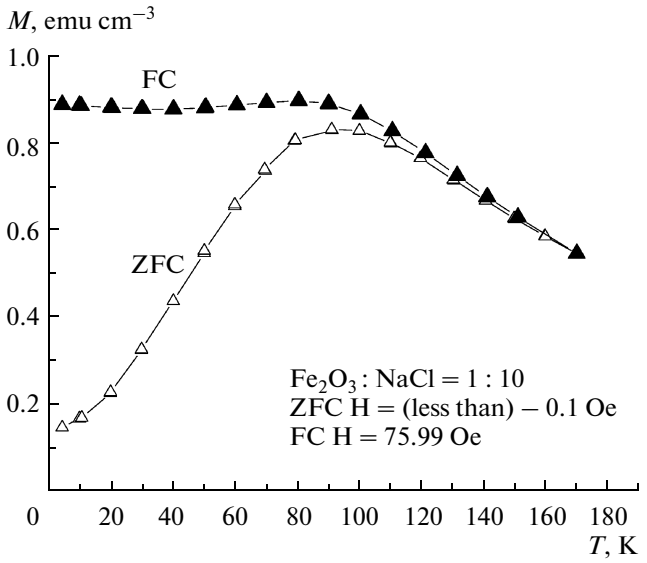

Fig. 4. Experimental relationships between magnetic moments and temperature for maghemite nanoparticles with an Fe_2O_3 : NaCl ratio of 1 : 10, determined upon cooling in a zero magnetic field (ZFC) and a constant magnetic field (FC) with an intensity of 76 Oe.

However, a magnetization temperature for maghemite has been given in a number of works (mainly geological) and proven to be quite adequate [13].

Our results for $M(H)$ allow us to calculate M from approximation according to [14] using the Langevin formula

$$\begin{aligned}\langle M\rangle &= \mu_{\text{eff}}/VL(\mu_{\text{eff}}H/kT)\\ &= M_s[\coth(\mu_{\text{eff}}H/kT) - kT/\mu_{\text{eff}}H],\end{aligned} \quad (1)$$

where V is a magnetic nanoparticle's volume; $L(x)$ is the Langevin function; $\mu_{\text{eff}} \sim 10^3$–$10^5$ is the magnetic moment per one cluster (nanoparticle), specifically $\mu_{\text{eff}} = 5700\ \mu_B$. The authors of [15], which was devoted to the magnetic properties of maghemite nanocrystals (mean size $d = 6.4$ nm, determined from X-ray broadening) and where similar problems were discussed, gave magnetic moment $\mu_{\text{eff}} = 8000\ \mu_B$ per one cluster and blocking temperature $T_B \simeq 101$ for fields $H =$ 50 Oe, which agrees with our experimental data. Experimental results for $M(T)$, obtained using the SQUID magnetometer, enabled us to calculate the relationship between magnetic susceptibility and temperature $\chi(T)$ (Fig. 3). Approximations using the Bloch formula $M(T) = N\mu_s[1 - (kT/A)^{3/2})]$ and relation $M(T) = N\mu_s[1 - (kT/B)^{4/3})]$ allow us to estimate Curie temperature T_C by extrapolating $\chi(T)$ to zero. For our nanoparticles, $T_C = 545$ K (with an error of 10 K); this is much lower than for bulk maghemite (918 K) [10]. At low temperatures, relation $M(T)$ is virtually linear, and at temperatures higher than 250 K it becomes a power relation. We did not observed the sharp ferromagnetic–paramagnetic transition near the Curie temperature that is typical of bulk samples.

The Curie temperature is significantly lower in maghemite nanoparticles with sizes of about several nanometers [16], due apparently to competition between super-exchange interactions of Fe^{3+} ions in tetrahedral and octahedral crystallographic positions at extremely small sizes (around several atomic layers). This has been confirmed by calculations using the Monte Carlo method [17].

Our samples of γ-Fe_2O_3 in the salt matrix differed in the ratio between the molar masses of the ferromagnetic ($M_{Fe_2O_3}$) and the salt capsule (M_{NaCl}) (Fig. 1b), i.e., as a result of the nanoparticle coating varying its magnetic properties. Figures 4 and 5 show the results obtained with the SQUID magnetometer for γ-Fe_2O_3 nanoparticles in the salt matrix at different ratios between $M_{Fe_2O_3}$ and M_{NaCl}. Experimental results for $M(T)$ were obtained under two measurement conditions: cooling in an external magnetic field (FC) and in a zero magnetic field (ZFC). With FC curves, there is typically a plateau below blocking temperature T_B that freezes the superparamagnetic moments of very small magnetic nanoparticles as in the spin–glass state in an amorphous magnetic. The relationship between temperature and magnetic moment for γ-Fe_2O_3 nanoparticles at low temperatures confirms the superparemagnetic behavior of the above nanoparticles (Fig. 4). The maximum temperature in the relation for a magnetic moment (Fig. 4) upon cooling in a zero field (ZFC) enables us to estimate the mean size of the nanoparticles. The blocking temperature [18] correlates with the size of a magnetic nanoparticle. It should be noted that this method does not consider the contribution to magnetization from the material's surface.

Figure 5 shows ZFC and FC curves measured for samples with different molar ratios between Fe_2O_3 and

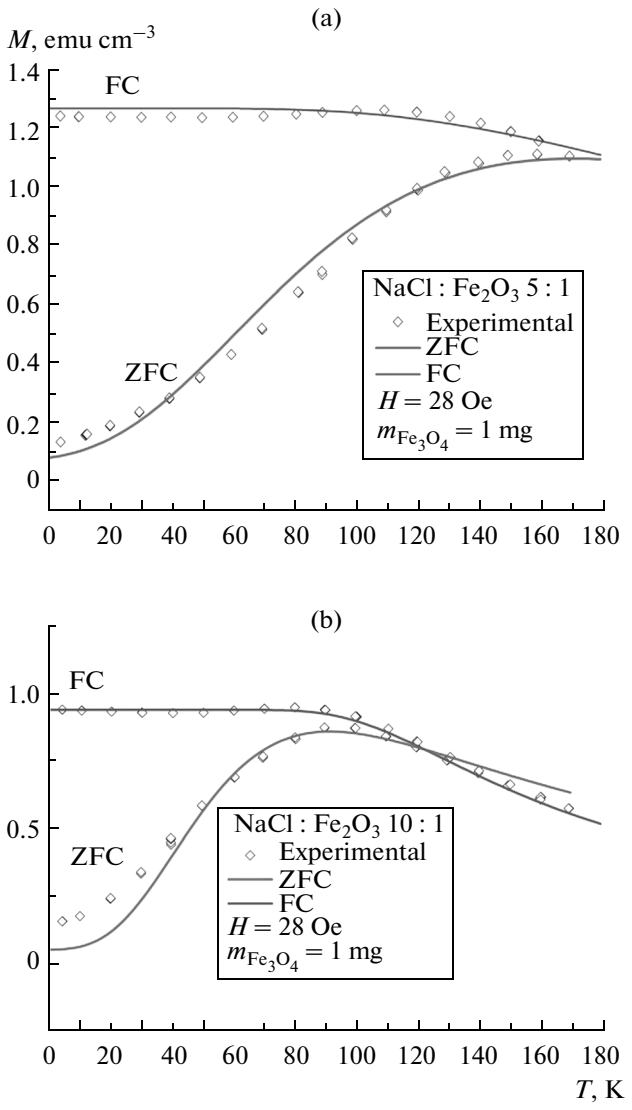

Fig. 5 Points are experimental values of magnetic moment; curves are the results from mathematically processing the temperature dependences of ZFC and FC for samples with molar Fe_2O_3 : NaCl ratios of (a) 1 : 5 and (b) 1 : 10.

NaCl, specifically 1 : 5 and 1 : 10. The mass of the magnetic material (maghemite) in the samples was the same. The difference between curves can be explained by interparticle interaction changing the blocking temperature, and by the slight difference in particle size resulting from specific features of the synthesis procedure.

RESULTS AND DISCUSSION

To analyze our results, we used a mathematical model that incorporated the ideas presented in [19]. For a monodispersed distribution of magnetic nanoparticles, the magnetic moment for ZFC and FC processes at super-magnetic approximations can be written as

$$M_{\mathrm{ZFC}} = \begin{cases} \dfrac{M_s^2 H}{3\mathrm{K}}, & T < T_b \\ M_s L\left(\dfrac{M_s V N}{kT}\right), & T > T_b. \end{cases} \quad (2)$$

In a polydispersed system, more blocked particles transition to the superparamagnetic state if the temperature is increased, and there is competition between two factors: particle unblocking (magnetization is increased still more) and relaxation of already unblocked (superparamagnetic) particles. At the moment ZFC reaches $T_{\max}$, the rate of magnetization relaxation of superparamagnetic particles starts to predominate over the rate of magnetization caused by new unblocked particles, and magnetization decreases if the temperature is raised still more. It is this relationship that is presented in Figs. 4 and 5.

With a polydispersed system of nanoparticles, we must consider the particles' distribution over size. As a result, Eq. (2) is transformed into

$$M_{\mathrm{ZFC}}(T) = \frac{M_s^2 H}{3K_V}\int_{V_b}^{\infty} V f(V)dV + \frac{M_s^2 H}{3kT}\int_0^{V_b} V^2 f(V)dV. \quad (3)$$

The following relationship was obtained for a monodispersed system in [15]:

$$M_{\mathrm{FC}} = \begin{cases} 30 \times \dfrac{M_s^2 H}{3K}, & T < T_b \\ M_s L\left(\dfrac{M_s V H}{kT}\right), & T > T_b, \end{cases} \quad (4)$$

By analogy with (3), for a polydispersed system we can write

$$M_{\mathrm{FC}}(T) = 30 \times \frac{M_s^2 H}{3K_V}\int_{V_b}^{\infty} V f(V)dV + \frac{M_s^2 H}{3kT}\int_0^{V_b} V^2 f(V)dV. \quad (5)$$

If we compare (2)–(5), we see that $M_{\mathrm{FC}} \geq M_{\mathrm{ZFC}}$, always. An equal sign would correspond to a situation in which all particles are unblocked.

The parameters of our model are M_s, $\langle r\rangle$ and σ_r (the saturation magnetization of a particle and its mean size and dispersion) for an isothermal curve of magnetization (Fig. 2) and M_s, $\langle V\rangle$, σ_V (the saturation magnetization of a particle, its mean volume, and volume dispersion) for curves ZFC and FC (Fig. 5). These

Maghemite parameters

γ-Fe_2O_3 : NaCl	$\langle d \rangle$, nm	σ	M_s, emu/cm^3	$\langle d_{Tmax} \rangle$, nm	$\langle d_{Keff} \rangle$, nm	M_{sKeff}, emu/cm^3	$\langle d_{TEM} \rangle$, nm
1 : 5 ZFC/FC	26	0.13	19/15	30	12.7	53/42	10
1 : 10ZFC/FC	21.8	0.11	23/19	25	10.7	61/49	
1 : 20ZFC/FC	21.6	0.13	23/19	27	10.5	65/53	
1 : 10M(H)	10	0.06	19				

parameters are used for fitting. The best agreement between calculated curves (2), (4) and the experimental results (Fig. 5) is observed for the parameters presented in the table.

For comparison, we present in the table the mean size of the particles obtained using the relationship between temperature and magnetic moment for ZFC conditions at maximum position $\langle d_{Tmax} \rangle$. The relationship between magnetization and temperature $M(T)$ for ZFC conditions and for FC conditions in this case differ greatly. ZFC magnetization increases monotonically if the temperature is raised, while FC magnetization varies little and the splitting of the ZFC–FC magnetization curves has its maximum near blocking temperature T_B. Blocking temperature T_B allows us to estimate the size of magnetic nanoparticles [18] according to the relation $K = 25k_BT_B/V$, where k_B is the Boltzmann factor and V is the volume of one nanoparticle. Values V determined using this procedure enable us to calculate $\langle d_{Tmax} \rangle$; our results are presented in the table. The table also gives particle sizes $\langle d_{TEM} \rangle$ obtained via transmission electron microscopy and laser correlation microscopy.

It can be seen that the mean particle sizes obtained through ZFC and FC measurements are approximately two times higher than those obtained using transmission electron microscopy $\langle d_{TEM} \rangle$. This was likely due to the surface anisotropy of the particles, which was not considered in mathematical processing according to (2) and (4). At the same time, the magnitude of surface magnetization is not important for the isothermal magnetization curve, since all particles are superparamagnetic if measurements are performed at room temperature.

CONCLUSIONS

There is a great difference between the magnetic properties of maghemite in the form of nanoparticles and bulk material. The relationship between temperature and magnetization is virtually linear and descending; extrapolation yields a Curie temperature of 545 K, which is considerably lower than the value for bulk samples. This effect is due to the competition between superexchange interaction between ions Fe^{3+} in the tetrahedral and octahedral crystallographic positions under conditions of supersmall sizes of around several atomic layers, as was confirmed by calculations performed using the Monte Carlo method [17]. The magnetic field dependences describing the temperature dependences of magnetization under different conditions of sample cooling yield rational estimates of nanoparticle size.

ACKNOWLEDGMENTS

This work was supported by the Ural Branch of the Russian Academy of Sciences, project no. 12-T-2-1001 (“Quantum Macrophysics and Nonlinear Dynamics”); by the Russian Foundation for Basic Research, project no. 14-02-92019 (“Physical and Chemical Mechanisms of Nanoparticle Interaction”); and by the Presidium of the Russian Academy of Sciences, project no. 12-P-2-1041 (“Quantum Mesoscopic and Disordered Structures”).

REFERENCES

1. Skaat, H. and Margel, S., *Biochem. Biophys. Res. Commun.*, 2009, vol. 386, no. 4, p. 645.
2. Nikiforov, V.N., *Nauka Tekhnol. Prom.*, 2011, no. 1, p. 90.
3. Jorgensen, F., *The Complete Handbook of Magnetic Recording*, New York: McGraw-Hill, 1996.
4. Keefer, C.M. and Shive, P.N., *Earth Planet. Sci. Lett.*, 1980, vol. 51, p. 199.
5. Keefer, C.M. and Shive, P.N., *J. Geophys. Res.*, 1981, vol. 86, p. 987.
6. Dunlop, D.J. and Özdemir, Ö., *Rock Magnetism: Fundamentals and Frontiers,* New York: Cambridge Univ. Press, 1997, vol. 3.
7. Gendler, T.S., Shcherbakov, V.P., Dekkers, M.J., et al., *Geophys. J. Int.,* 2005, vol. 160, p. 815.
8. Özdemir, Ö. and Banerjee, S.K., *Geophys. Res. Lett.*, 1984, vol. 11, p. 161.
9. Özdemir, Ö., *Phys. Earth Planet. Int.*, 1990, vol. 65, p. 125.

10. Liu, X.M., Shaw, J., Jiang, J.Z., et al., *Sci. China Earth Sci.*, 2010, vol. 53, p. 1153.

11. Chekanova, A.E., Sorkina, T., Nikiforov, V.N., et al., *Mendeleev Commmun.,* 2009, vol. 19, p. 1.

12. Chekanova, A.E., Biocompatible magnetic nanomaterials based on ferrum (III) oxides, *Extended Abstract of Cand. Sci. (Chem.) Dissertation*, Moscow: MSU, 2008.

13. Bowles, J.F., Howie, R.A., Vaughan, D.J., and Zussman, J., *Rock-Forming Minerals*, vol. 5: *Non-Silicates: Oxides, Hydroxides and Sulphides*, London: Geological Soc. London, 2011.

14. Nikiforov, V.N., Oxengendler, B.L., Turaeva, N.N., et al., *J. Phys.: Conf. Ser.*, 2011, vol. 291, p. 012009.

15. Manivannan, A., Seehra, M.S., Shah, N., and Huffman, G.P., *Phys. Rev. B*, 2004, vol. 70, p. 174428.

16. Nikiforov, V.N., Koksharov, Yu.A., Polyakov, S.N., et al., *J. Alloys Compounds*, 2013, vol. 569, p. 58.

17. Restrepo, J., Labaye, Y., and Greneche, J.M., *Revista de la Sociedad Colombiana de Fisica*, 2006, vol. 38, p. 1559.

18. Gubin, S.P., Koksharov, Yu.A., Khomutov, G.B., and Yurkov, G.Yu., *Usp. Khim.*, 2005, vol. 74, no. 6, p. 539.

19. Sappey, R., Vincent, E., Hadacek, N., et al., *Phys. Rev. B,* 1997, vol. 56, no. 22, p. 14551.

Translated by Yu. Zikeeva